

Original Paper

# Mitochondrial Network and Biogenesis in Response to Short and Long-Term Exposure of Human BEAS-2B Cells to Aerosol Extracts from the Tobacco Heating System 2.2

Jarosław Walczak<sup>a</sup> Dominika Malińska<sup>a</sup> Karolina Drabik<sup>a</sup> Bernadeta Michalska<sup>a</sup>  
Monika Prill<sup>a</sup> Stephanie Johne<sup>b</sup> Karsta Luettich<sup>b</sup> Jędrzej Szymański<sup>a</sup>  
Manuel C. Peitsch<sup>b</sup> Julia Hoeng<sup>b</sup> Jerzy Duszyński<sup>a</sup> Mariusz R. Więckowski<sup>a</sup>  
Marco van der Toorn<sup>b</sup> Joanna Szczepanowska<sup>a</sup>

<sup>a</sup>Nencki Institute of Experimental Biology, Polish Academy of Sciences, Warsaw, Poland, <sup>b</sup>PMI R&D, Philip Morris Products S.A., Neuchâtel, Switzerland

## Key Words

Mitochondrial dynamics • Candidate modified risk tobacco product • Tobacco Heating System 2.2 • BEAS-2B cells • Cigarette smoke

## Abstract

**Background/Aims:** Adverse effects of cigarette smoke on health are widely known. Heating rather than combusting tobacco is one of strategies to reduce the formation of toxicants. The sensitive nature of mitochondrial dynamics makes the mitochondria an early indicator of cellular stress. For this reason, we studied the morphology and dynamics of the mitochondrial network in human bronchial epithelial cells (BEAS-2B) exposed to total particulate matter (TPM) generated from 3R4F reference cigarette smoke and from aerosol from a new candidate modified risk tobacco product, the Tobacco Heating System (THS 2.2). **Methods:** Cells were subjected to short (1 week) and chronic (12 weeks) exposure to a low (7.5 µg/mL) concentration of 3R4F TPM and low (7.5 µg/mL), medium (37.5 µg/mL), and high (150 µg/mL) concentrations of TPM from THS 2.2. Confocal microscopy was applied to assess cellular and mitochondrial morphology. Cytosolic Ca<sup>2+</sup> levels, mitochondrial membrane potential and mitochondrial mass were measured with appropriate fluorescent probes on laser scanning cytometer. The levels of proteins regulating mitochondrial dynamics and biogenesis were determined by Western blot. **Results:** In BEAS-2B cells exposed for one week to the low concentration of 3R4F TPM and the high concentration of THS 2.2 TPM we observed clear changes in cell morphology, mitochondrial network fragmentation, altered levels of mitochondrial fusion and fission

proteins and decreased biogenesis markers. Also cellular proliferation was slowed down. Upon chronic exposure (12 weeks) many parameters were affected in the opposite way comparing to short exposure. We observed strong increase of NRF2 protein level, reorganization of mitochondrial network and activation of the mitochondrial biogenesis process. **Conclusion:** Comparison of the effects of TPMs from 3R4F and from THS 2.2 revealed, that similar extent of alterations in mitochondrial dynamics and biogenesis is observed at 7.5 µg/mL of 3R4F TPM and 150 µg/mL of THS 2.2 TPM. 7 days exposure to the investigated components of cigarette smoke evoke mitochondrial stress, while upon chronic, 12 weeks exposure the hallmarks of cellular adaptation to the stressor were visible. The results also suggest that mitochondrial stress signaling is involved in the process of cellular adaptation under conditions of chronic stress caused by 3R4F and high concentration of THS 2.2.

© 2020 The Author(s). Published by  
Cell Physiol Biochem Press GmbH&Co. KG

## Introduction

Tobacco smoke-induced inflammation, epithelial injury, and cell death are major causative factors in airway diseases, such as chronic obstructive pulmonary disease and lung cancer [1, 2]. Tobacco smoke contains thousands of harmful and potentially harmful constituents (HPHC) that affect cellular metabolism [3].

Mitochondria play a key role in cellular metabolism given that they synthesize adenosine triphosphate (ATP) by oxidative phosphorylation, providing cellular energy [4]. Mitochondria also buffer calcium ions and are essential for cellular functions such as growth, division, and apoptosis [5, 6]. Impaired mitochondrial function leads to defects in mitochondrial energy production, mitochondrial dynamics, and mitochondrial signaling [7]. The sensitive nature of mitochondrial dynamics makes mitochondria early indicators of cellular stress. As such, mitochondrial dysfunction has been recognized as a key component in acute and chronic cellular stress [8], and it has been associated with numerous multisystem syndromes, such as neurodegenerative disorders, cancer, and aging [9–11].

Mitochondria form dynamic network maintained by the opposing processes of fission and fusion [4], which affect mitochondrial bioenergetics, ATP production and apoptosis [12–14]. Therefore, the tight regulation of mitochondrial dynamics is vital for maintaining mitochondrial functions [4]. Remodeling of outer and inner mitochondrial membranes controls mitochondrial shape and affects the balance of fusion and fission processes [15]. Fission provides a mechanism to isolate the damaged components during normal lifespan or during increased oxidative stress for elimination. Mitochondrial fission is mediated by proteins, such as dynamin-related protein 1 (Drp1), fission 1 (Fis1), mitochondrial fission factor (Mff), and mitochondrial dynamic proteins (49 and 51 kDa) (MiD49/51) [16, 17]. For mitochondrial fusion, the critical protein is optic atrophy 1 (OPA1), a member of the dynamin family of GTPases located in the mitochondrial intermembrane space, where it is involved in the maintenance of mitochondrial cristae remodeling and inner membrane fusion [18]. OPA1 is processed into eight isoforms. Changes in the balance between these isoforms affect mitochondrial fusion [19, 20] and can also affect respiratory chain activity and mitochondrial metabolism [21]. Fusion controls mitochondrial morphology and maintains mitochondrial function, including membrane potential and oxidative phosphorylation, by permitting the exchange of mtDNA, proteins, and metabolites. The sensitive homeostatic balance of fusion and fission dynamics is emerging as a critical upstream determinant of the cellular stress response. Mitochondrial biogenesis process is activated as part of the mitochondrial stress response pathway. This process allows for the maintenance of cellular and organismal homeostasis and enhanced cell survival and stress resistance. Because mitochondrial abundance, integrity, activity, and morphology are fundamental for cell life, mitochondrial impairment can disrupt various cellular functions and initiate events that result in the onset of diseases.

In this study, we investigated alterations of the dynamics of the mitochondrial network and mitochondrial biogenesis following exposure to two types of total particulate matter (TPM) generated from 1) aerosol from a new candidate modified risk tobacco product (cMRTP), the Tobacco Heating System (THS) 2.2, and 2) smoke from a 3R4F reference cigarette. This new cMRTP, THS 2.2, heats tobacco instead of burning it. The dominant constituents in heat-not-burn aerosols are generated by evaporation and distillation processes [22]. Combustion is eliminated, and tobacco pyrolysis is reduced to a minimum, thus significantly reducing the emission of many constituents identified as toxicants [23]. Many HPHCs are present in TPM [24]. Therefore, in this study, TPM was used as a test item to investigate the effects of the mixture of chemicals present in CS on mitochondrial stress response (mitochondrial morphology and dynamics) in human bronchial epithelial cells *in vitro* and to compare these effects with those of the TPM from THS 2.2 aerosol. To compare the impact of exposure to THS 2.2 aerosol and 3R4F cigarette smoke TPM, we conducted short-term (one week) and chronic (12 weeks) assessments using human bronchial epithelial cells (BEAS-2B) exposed directly to TPM. Further, we studied the alterations of different transcription factors and mitochondrial mass to determine the type of mitochondrial stress induced by tobacco-related HPHCs.

## Materials and Methods

### *Chemicals and antibodies*

Fluo-4 AM, JC-1, MitoTracker® Green, and 4',6-diamidino-2-phenylindole (DAPI) were acquired from Invitrogen (Carlsbad, CA, USA). Paraformaldehyde, saponin, ionomycin, and thapsigargin were from Sigma Aldrich (St. Louis, MO, USA), and fetal bovine serum (FBS) was from Gibco Thermo Fisher Scientific (Waltham, MA, USA). All chemicals were of analytical grade and purchased from various suppliers, as indicated. Primary antibodies against Drp1, phosphorylated at serine 616, TFAM, and Mfn2, were obtained from Cell Signaling Technology (Danvers, MA, USA); antibodies against Drp1 and OPA1 were from BD Biosciences (San Jose, CA, USA). An anti-GAPDH antibody was obtained from Merck Millipore (Billerica, MA, USA). Anti-Fis1 and mouse anti- $\beta$ -actin antibodies were purchased from Sigma-Aldrich (St. Louis, MO, USA), and Mff, Mfn1, rabbit  $\beta$ -actin, NRF1, and NRF2 antibodies were from Abcam (Cambridge, UK). Rabbit and mouse fluorescently labelled secondary antibodies IRDye®680LT and IRDye®800CW were from LI-COR Biosciences (Lincoln, NE, USA).

### *Generation of 3R4F and THS 2.2 TPM*

The 3R4F reference cigarettes were purchased from the University of Kentucky (Lexington, KY, USA; <http://www.ca.uky.edu/refcig/>), and tobacco stick holders were provided by Philip Morris Products S.A. (Neuchâtel, Switzerland). The 3R4F and THS 2.2 sticks were kept at  $22 \pm 1^\circ\text{C}$  and  $60\% \pm 3\%$  relative humidity for a minimum of 48 hours, as per ISO Standard 3402 (International Organisation for Standardization; 2010). Once inserted in the holder, which includes a battery, controls, and a heating element, the THS 2.2 stick was heated and subsequently emitted an aerosol comprising water, glycerin, nicotine, and flavors [23]. A 20-port Borgwaldt smoking machine (Hamburg, Germany) was used to generate smoke from 3R4F cigarettes, and a 30-port SM2000/P1 smoking machine (Philip Morris International, Neuchâtel, Switzerland) drew aerosol from THS 2.2, as per the Health Canada Intense protocol (55 mL puff volume; 2-second puff duration; 2 puffs/min; 100% blocking of 3R4F filter ventilation holes; Health Canada, 1999). TPM from 3R4F reference cigarette mainstream smoke or THS 2.2 aerosol was trapped on Cambridge glass fiber filter pads and then extracted with an appropriate volume of dimethyl sulfoxide (DMSO) to yield a final concentration of 100 mg TPM/mL.

## *Cell culture and exposure*

The BEAS-2B human bronchial epithelial cell line was obtained from the American Type Culture Collection (ATCC, Manassas, VA, USA). A mycoplasma test was carried out by Public Health England (Salisbury, UK). Cell line authentication was performed by ATCC using the short tandem repeat profiling method. BEAS-2B cells were cultured in bronchial epithelial cell growth medium (BEGM™) consisting of bronchial epithelial basal medium (BEBM™) supplemented with a SingleQuots™ kit (Lonza, Basel, Switzerland). Cells were seeded on culture plates coated with type I collagen and maintained in the incubator at 37°C in 5% CO<sub>2</sub>. The BEAS-2B cells were exposed to TPM through continuous culturing for 1 or 12 weeks in a cell growth medium containing TPM from 3R4F cigarette smoke at low concentration (7.5 µg/mL) or at low, medium and high concentration of TPM from THS 2.2 aerosol (7.5, 37.5, and 150 µg/mL, respectively). Because TPMs were extracted with DMSO the vehicle control was also included by the culturing cells for 1 or 12 weeks with the growth medium containing DMSO at concentration corresponding to the one used for the TPM exposure (0.1 %). Due to the long incubation time with TPM, when the cells required a change of growth medium or passage, fresh culture medium containing TPMs or DMSO at appropriate concentration was used. Cells were then collected for further assessment.

Starvation of the cells was induced by incubation with PBS (with ions of calcium and magnesium at concentrations 0.9 mM and 0.5 mM, respectively) for 24 hours.

## *BEAS-2B cell proliferation during one-week exposure to TPM*

On the first day of the experiment, cells were seeded into three 24-well plates (4,000/well) and six 100 mm culture plates (8\*10<sup>5</sup> cells/culture plate). Four hours after seeding, cells were exposed to 7.5 µg/mL 3R4F TPM or to 7.5, 37.5, or 150 µg/mL THS 2.2 TPM. Cells were detached from plates 24, 48, and 72 hours after seeding using Accutase™ (Gibco, Thermo Fisher Scientific, Waltham, MA, USA), stained with 0.4 % Trypan Blue solution (Sigma-Aldrich, St. Louis, MO, USA) and manually counted under a microscope using a Neubauer counting chamber. Seventy-two hours after seeding, cells from the 100 mm culture plates were re-seeded onto four 24-well plates at a density of 20,000 cells per well. Four hours after re-seeding, cells were treated with TPM. Over the next four days, cell numbers were counted. The number of cells ( $N$ ) relative to the number of cells on the first day after seeding ( $N_0$ ) was calculated as a function of time. Results were fitted with the exponential growth model  $N/N_0 = 2^{ft}$ , where  $t$  is the time in days and  $f$  is the frequency of cell cycles per day.

## *Whole-cell extracts and immunoblotting*

Cells grown in 75-cm<sup>2</sup> culture flasks were harvested using Accutase™, rinsed with ice-cold phosphate-buffered saline (PBS), collected by centrifugation, and resuspended in RIPA lysis buffer supplemented with protease and phosphatase inhibitor cocktails (all Sigma-Aldrich, St. Louis, MO, USA). Cells were incubated in lysis buffer on ice for 20 minutes. Cell lysates were then homogenized and centrifuged at 16,000 ×  $g$  for 20 minutes. The supernatants were collected, and protein concentrations were determined according to the Bradford method (Bradford, 1976). The samples were supplemented with sodium dodecyl sulfate (SDS) sample buffer (0.5 M Tris-HCl, 2.3% SDS, 5% mercaptoethanol [v/v], 12.5% glycerol [v/v]; pH 6.8). Lysates containing equal amounts of protein (10–50 µg) were separated by SDS-polyacrylamide gel electrophoresis, transferred to nitrocellulose or polyvinylidene difluoride membranes (Bio-Rad Laboratories, Hercules, CA, USA), and blocked using Odyssey blocking buffer (LI-COR Biosciences, Lincoln, NE, USA), diluted 1:1 in Tris-buffered saline for one hour. Blots were incubated overnight with primary antibodies at following dilutions: Drp1, phosphorylated at serine 616 – 1:1,000; TFAM – 1:1,000; Mfn2 – 1:1,000; Drp1 – 1:1,000; OPA1 – 1:1,000; GAPDH – 1:20,000; Fis1 – 1:1,000; mouse anti-β-actin – 1:150,000; Mff – 1:1,000; Mfn1 – 1:1,000; rabbit β-actin – 1:100,000; NRF1 – 1:1,000; and NRF2 – 1:1,000. Subsequently, blots were rinsed with PBS-0.1% Tween 20 and incubated with fluorescently labelled secondary antibodies, diluted 1:10,000 in Odyssey blocking buffer, for one hour. The fluorescent signal on the membrane was measured using an Odyssey infrared imaging system (LI-COR Biosciences, Lincoln, NE, USA).

### *Live cell studies*

Seventy-two hours before the end of one or 12-week exposure, cells were seeded onto 24-well plates at a density of 3, 500–7, 000 cells per well. Seeding density was individually adjusted for each exposure concentration to account for differences in proliferation so that at the time of measurement, all cells had a similar confluence (approximately 80%). Next, cells were loaded with fluorescent probes (see below), rinsed twice with fresh PBS, and 0.5 mL of fresh PBS was then added to each well prior to measurements using an iCys Laser Scanning Cytometer (Thorlabs Inc., Newton, NJ, USA) at 20× magnification. Nine to 12 fields of view were captured and analyzed from each well. A single field of view corresponded to 500 × 384 μm in the format of 1, 000 × 768 pixels.

### *Cytosolic Ca<sup>2+</sup> levels*

Cells were loaded with 4 μM of fluo-4 AM dye in PBS with 5.56 mM glucose at 37°C for 30 minutes. The intensity of the probe fluorescence was measured at excitation and emission wavelengths of 488 nm and 530 nm, respectively, using a 530/30-nm filter cube. As a positive control, after loading and washing out the probe, selected wells were additionally exposed to 3 μM ionomycin or 2 μM thapsigargin for 10 minutes [25, 26].

### *Mitochondrial membrane potential*

Cells were loaded with 5 μM of JC-1 dye in PBS at 37°C for 30 minutes. This compound accumulates in the mitochondrial matrix proportionally to the electric potential established on the inner mitochondrial membrane and can aggregate in the matrix when at higher concentrations. The aggregates emit red fluorescence (emission max. 590 nm), whereas the fluorescence of JC-1 monomers is green (emission max. 527 nm). The probe fluorescence was measured at 488 nm and 530 nm excitation and emission wavelength, respectively, for JC-1 monomers, or 580 nm emission wavelength for JC-1 aggregates, using 530/30 nm filter cubes (green channel) or 580/30 nm filter cubes (orange channel).

### *Mitochondrial mass*

Cells were loaded with 100 nM of MitoTracker™ Green dye in PBS at 37°C for 15 minutes. The probe fluorescence was measured at excitation and emission wavelengths of 488 nm and 530 nm, respectively, using a 530/30 nm filter cube. MitoTracker™ Green contains a mildly thiol-reactive chloromethyl moiety and it accumulates in the mitochondrial matrix regardless of mitochondrial membrane potential, where it binds to free thiols on mitochondrial proteins.

### *Analysis of laser scanning cytometry data*

Captured images were analyzed using the iCys software version 2.5 to quantify the fluorescence signal originating from the fluorescent probes. Each microscopy image was divided into smaller regions (phantom contours) in which the fluorescent signal was quantified. Based on the histogram of the obtained phantom intensities, different areas of the image corresponding to the signal and background were identified. The radius of the applied phantom contours was in the range of 1–2 μm. The average number of detected phantom contours per well was in the order of 10<sup>4</sup>–10<sup>5</sup>, corresponding to several hundred (10<sup>2</sup>–10<sup>3</sup>) cells. For the MitoTracker™ Green and fluo-4 AM dyes, the signal from the whole cell area was integrated. For the JC-1 dye, the signal was quantified in the orange and green channels, and the ratio of the orange to green intensities (ratio of JC-1 aggregates to JC-1 monomers) was calculated. For each fluorescent probe, the background-corrected signal was averaged over several wells, and the measured intensity was normalized to mean values obtained in each experiment for unexposed cells (controls). At least three independent experiments using 24-well plates were averaged to obtain the results.

### *Immunocytochemical imaging and confocal image analysis*

Cells seeded on 12 mm diameter glass coverslips were fixed with 4% paraformaldehyde in PBS for 15 minutes at room temperature, rinsed with 10% FBS/PBS, and incubated with an anti-alpha-tubulin antibody in 10% FBS/PBS supplemented with 0.2% saponin for one hour. After rinsing three times with 10% FBS/PBS to remove unbound antibody, cells were incubated with Alexa Fluor 488 phalloidin or a secondary Alexa Fluor 488-conjugated antibody diluted in 10% FBS/PBS containing 0.2% saponin and DAPI for one hour.

Coverslips were washed three times with 10% FBS/PBS and once with PBS and then mounted on a slide with anti-fading mounting medium coating (Dako, Carpinteria, CA, USA).

To visualize the distribution of mitochondria, cells were incubated with 200 nM MitoTracker™ CMXRos in the dark at 37°C for 15 minutes. The cells were then rinsed with the medium and fixed. CMXRos is a cationic lipophilic dye; it is preferentially sequestered into mitochondria by forming covalent thioester bonds with thiols of proteins in the mitochondrial matrix [27]. Fluorescence microscopy was carried out using a Zeiss LSM780 confocal microscope (Carl Zeiss, Oberkochen, Germany) with a 63× oil immersion objective. Images were acquired from randomly selected fields of confluent and non-confluent cells.

Mitochondrial morphology within the cells was estimated by visual inspection based on microscopic images. Mitochondrial network was assigned to the one of the morphological subtypes:

Fragmented mitochondria – mitochondrial network is fragmented. There is no visible network; most of mitochondria form large, round and clustered puncta.

Other – mitochondrial network is partly fragmented, mostly in a distal part of the cell. Large, round, as well as puncta mitochondria are still present, but they are in a minority. Mitochondrial network is diminished and separated rods are visible.

Network – mitochondrial network is fused, with junctions and branches. Separated rods are in a minority, mostly in a distal part of the cell.

Subsequently the percentage content of each subtypes were counted for each treatment conditions or each conditions between 17 and 45 cells were taken to the analysis.

### *Statistical analysis*

Data are expressed as means ± standard deviation of values derived from at least three independent experiments (n = number of biological replicates). Statistical significance for comparisons between values obtained for cells exposed to TPM and untreated cells or vehicle controls was assessed using a Student's *t*-test. Only *p*-values lower than 0.05 were considered statistically significant.

## **Results**

### *Cell proliferation and mitochondrial physiology*

*Effects of short-term and chronic exposure to TPM from 3R4F cigarette smoke and THS 2.2 aerosol on cellular growth and architecture.* A characteristic element of cellular stress is inhibition of proliferation. As a result of severe stress, the morphology and shape of cells may also change. Incubation with TPM from 3R4F cigarette smoke or THS 2.2 aerosol for one to three days did not result in any significant differences in cell proliferation at days 1 and 2 compared with DMSO-exposed and control cells (Fig. 1A). We observed significant decreases in the growth rate of cells exposed to 7.5 µg/mL, 37.5 µg/mL, 150 µg/mL THS 2.2, and 7.5 µg/mL 3R4F TPM compared with DMSO-exposed cells at day 3 of exposure.

After re-passage of the cells, the exposure was continued up to four to seven days. Cells exposed to 37.5 µg/mL and 150 µg/mL THS 2.2 or to 7.5 µg/mL 3R4F TPM grew at a significantly slower rate than untreated control and DMSO-exposed cells. Cells exposed to 7.5 µg/mL THS 2.2 TPM and control cells grew at a rate similar to that of DMSO-exposed cells. On Day 7 of the experiment, the number of cells exposed to 3R4F (7.5 µg/mL) or THS 2.2 (150 µg/mL) TPM was approximately one-fourth the number of DMSO-exposed cells (Fig. 1B).

TPM from 3R4F cigarette smoke and THS 2.2 aerosol also affected cell morphology visualized by marked actin filaments (usually cortical localization within the cell) (Fig. 2A) and microtubules (usually located evenly in the body of the cell) (Fig. 2B). Cell shape differed among cells treated with 3R4F (7.5 µg/mL) or THS 2.2 (150 µg/mL) TPM for seven days vs. DMSO-exposed and control cells (Fig. 2A, B indicated by white arrows). Specifically, some of the cells exposed to TPM from 3R4F cigarette smoke or THS 2.2 aerosol (150 µg/ml) had an elongated and also small round shape, with cortically concentrated stress fibres of actin filaments (marked with an asterisks in Fig. 2).

**Fig. 1.** Effects of a one-week exposure of BEAS-2B cells to TPM from 3R4F reference cigarette smoke (7.5  $\mu\text{g}/\text{mL}$ ) and THS 2.2 aerosol (7.5  $\mu\text{g}/\text{mL}$ , 37.5  $\mu\text{g}/\text{mL}$ , and 150  $\mu\text{g}/\text{mL}$ ) on cell proliferation: (A) growth rate, (B) growth curve. Cells were counted every day during 7 days treatment. After 3 days cells were reseeded to new wells and the experiment was continued up to 7 days. Due to that the result are presented in 2 separate (left and right) graphs.

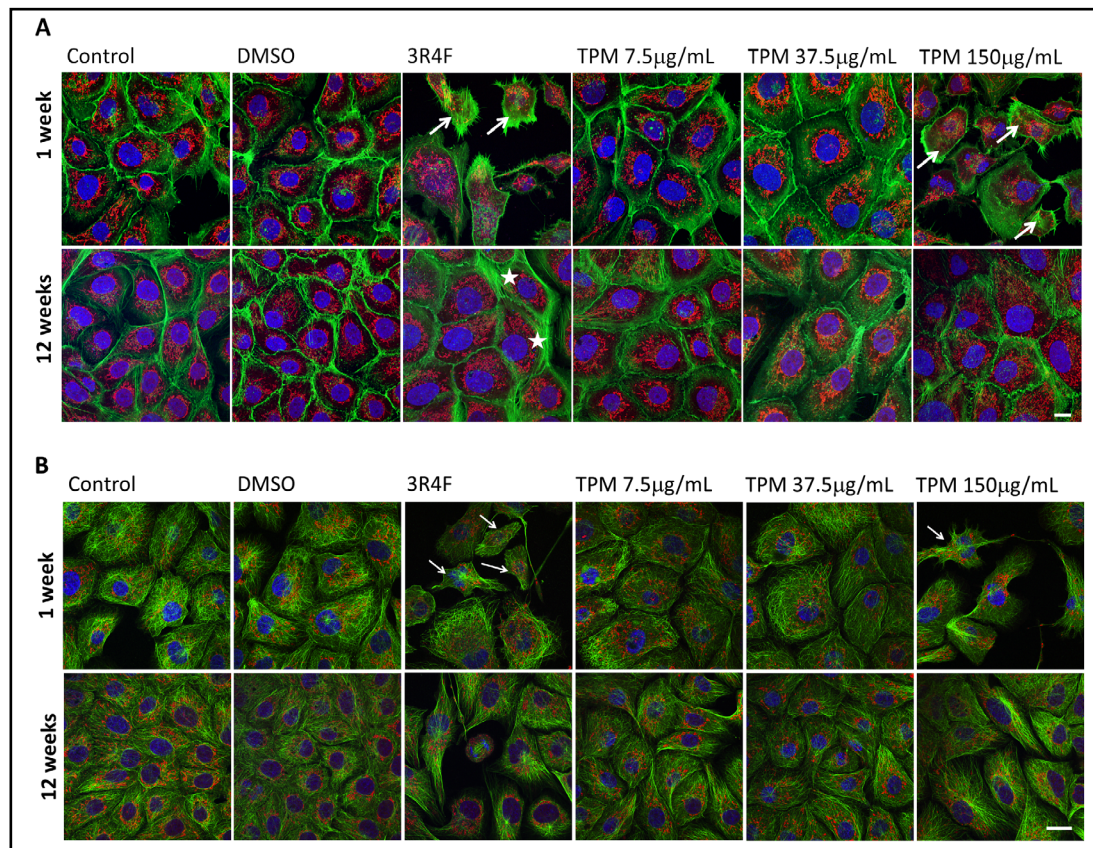
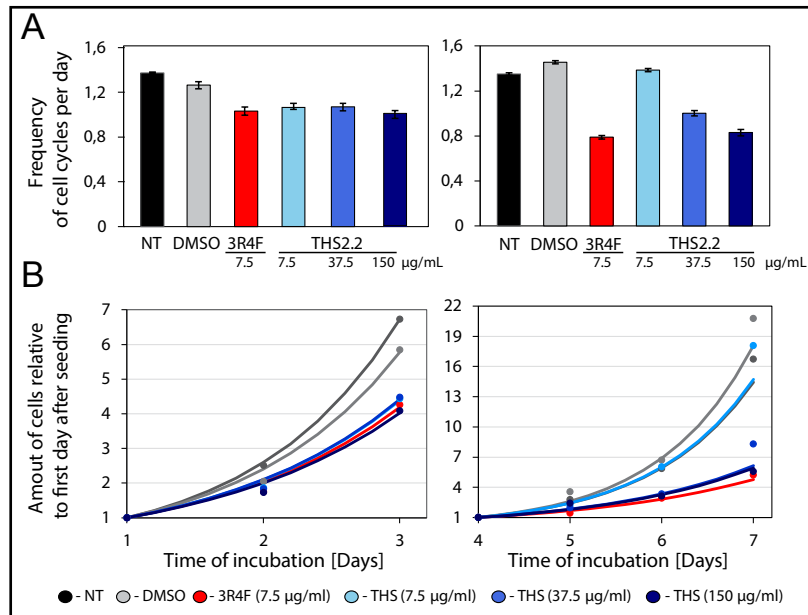


**Fig. 2.** Effects of one- and 12-week exposures of BEAS-2B cells to TPM from 3R4F reference cigarette smoke (7.5  $\mu\text{g}/\text{mL}$ ) and THS 2.2 aerosol (7.5  $\mu\text{g}/\text{mL}$ , 37.5  $\mu\text{g}/\text{mL}$ , and 150  $\mu\text{g}/\text{mL}$ ) on cellular morphology: (A) representative images of cellular architecture presented by actin filament staining (green), (B) representative images of cellular architecture presented by microtubules staining (green). Arrows - indicate distinct cells (shrunken cells), asterisks - clusters of stress fibers. Red, mitochondria; blue, nuclei. Scale bar represents 20  $\mu\text{m}$ .

Fig. 2 also shows the cellular morphology following 12 weeks of exposure. After 12 weeks of incubation, the shape of the cells (cultured in each condition) was similar to control cells, only more clusters of stress fibres were visible in cells exposed to 3R4F cigarette smoke aerosol (Fig. 2A, asterisks).

*Effects of short-term and chronic exposure to TPM from 3R4F cigarette smoke and from THS 2.2 aerosol on mitochondrial membrane potential and cytosolic calcium levels.* Mitochondrial membrane potential ( $\Delta\Psi_m$ ) is an indicator of general mitochondrial function. Mitochondrial membrane potential was slightly lower in cells exposed to 7.5  $\mu\text{g/mL}$  and 37.5  $\mu\text{g/mL}$  THS 2.2 TPM for seven days compared with that in DMSO-exposed cells (Fig. 3A). Twelve-week exposure to TPM from 3R4F (7.5  $\mu\text{g/mL}$ ) cigarette smoke and THS 2.2 (7.5  $\mu\text{g/mL}$ , 37.5  $\mu\text{g/mL}$ , and 150  $\mu\text{g/mL}$ ) aerosol had no effect on mitochondrial membrane potential (Fig. 3A).

Alterations in cellular and mitochondrial morphology are also associated with changes in intracellular calcium levels. One of the main function of mitochondria is  $\text{Ca}^{2+}$  buffering. Dysfunction of mitochondria can lead to disturbances in calcium buffering increasing its cytosolic concentration [28]. We therefore measured calcium levels in the cytosol of BEAS-2B cells. A one-week exposure to TPM from THS 2.2 aerosol caused a concentration-dependent elevation of cytosolic calcium level (Fig. 3B). The result, however, was only statistically significant for the highest concentration of THS 2.2 TPM, which raised calcium levels in the cytosol by  $23 \pm 15\%$  ( $n=4$ ). A significant increase of cytosolic calcium level by  $35 \pm 28\%$  was observed in cells exposed to TPM from 3R4F (7.5  $\mu\text{g/mL}$ ) smoke ( $n=4$ ; Fig. 3B). The maximal fluo-4 signal obtained following addition of the calcium ionophore ionomycin was similar in all treatment conditions (data not shown).

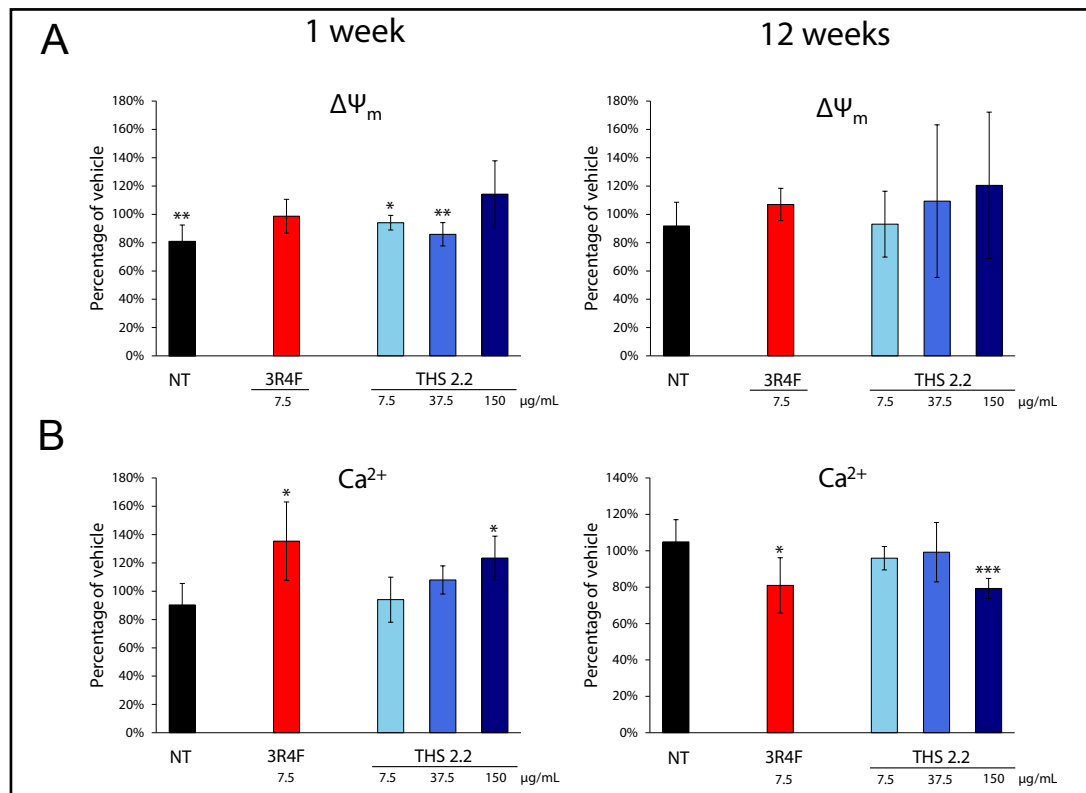


**Fig. 3.** Effects of one- and 12-week exposures of BEAS-2B cells to TPM from 3R4F reference cigarette smoke (7.5  $\mu\text{g/mL}$ ) and THS 2.2 aerosol (7.5  $\mu\text{g/mL}$ , 37.5  $\mu\text{g/mL}$ , and 150  $\mu\text{g/mL}$ ) on (A) mitochondrial membrane potential ( $\Delta\Psi_m$ ) measured using a JC-1 molecular probe and (B) cytosolic calcium levels measured using a Fluo-4 molecular probe. Values represent the means  $\pm$  SD from at least three independent experiments. \* $p < 0.05$ , \*\* $p < 0.01$ , \*\*\* $p < 0.001$  compared with vehicle (DMSO)-treated cells. NT, non-treated (control) cells.

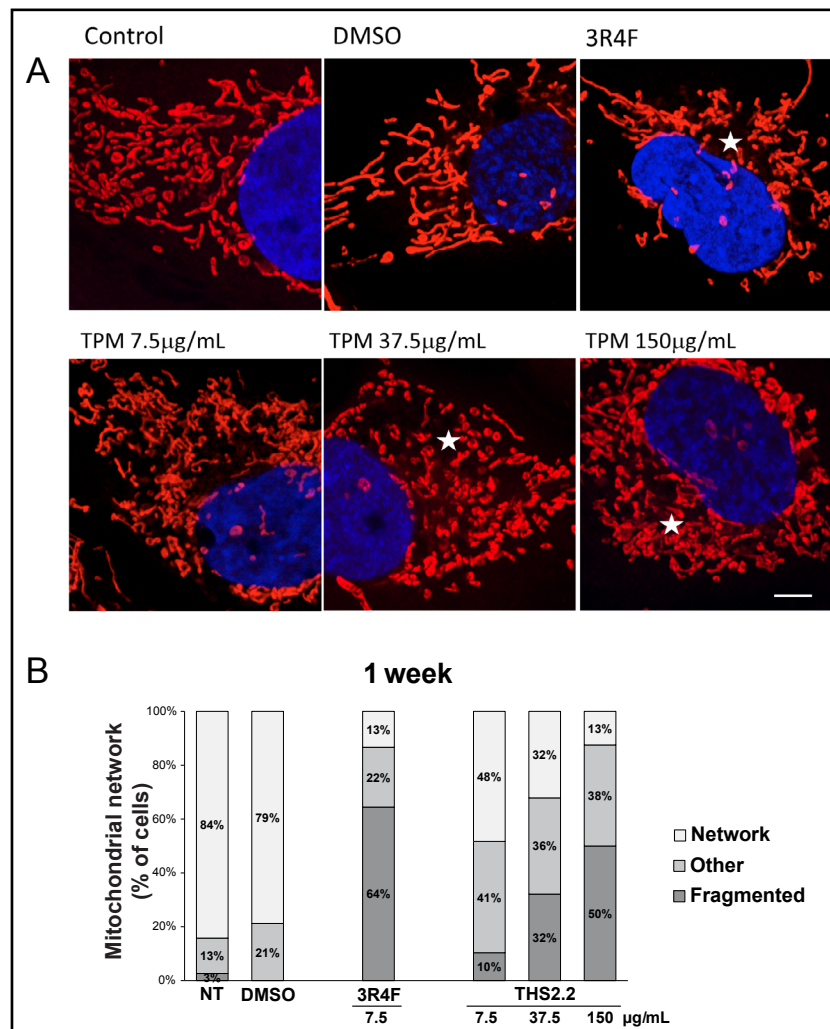
When cells were exposed for 12 weeks, changes in cytosolic calcium levels were milder. In cells exposed to TPM from 3R4F (7.5  $\mu\text{g}/\text{mL}$ ) cigarette smoke, cytosolic calcium level decreased by  $19 \pm 15\%$  compared with DMSO-treated cells ( $n=4$ ). Only exposure to the highest concentration of TPM from THS 2.2 (150  $\mu\text{g}/\text{mL}$ ) caused a statistically significant drop in the calcium levels measured ( $21 \pm 5\%$ ,  $n=4$ ; Fig. 3B).

#### Mitochondrial dynamics

*Effects of short-term and chronic exposure to TPM from 3R4F cigarette smoke and from THS 2.2 aerosol on mitochondrial network organization.* Appropriate distribution of the mitochondrial network is essential for cell survival and contributes to organelle function. In BEAS-2B cells, mitochondria tend to have an elongated -rod like shape and form an intracellular network. Typical mitochondrial organization within BEAS-2B cells is shown in Fig. 4 (images control cells). In cells incubated with TPM from 3R4F (7.5  $\mu\text{g}/\text{mL}$ ) cigarette smoke and THS 2.2 aerosol (37.5  $\mu\text{g}/\text{mL}$  and 150  $\mu\text{g}/\text{mL}$ ) for one week, mitochondrial shape varied from tubular to rounded and punctate. The mitochondrial network of these cells were more fragmented than in control cells, as marked by asterisks (Fig. 4A).

These observations were confirmed by quantification of mitochondrial network fragmentation presented on the graph in Fig. 4B. Exposure to the TPM from 3R4F (7.5  $\mu\text{g}/\text{mL}$ ) cigarette smoke (one week) caused fragmentation of mitochondrial network in almost 65% of cells while the same concentration of TPM from THS 2.2 aerosol led to mitochondrial

**Fig. 4.** Effects of a one-week exposure of BEAS-2B cells to TPM from 3R4F reference cigarette smoke (7.5  $\mu\text{g}/\text{mL}$ ) and THS 2.2 aerosol (7.5  $\mu\text{g}/\text{mL}$ , 37.5  $\mu\text{g}/\text{mL}$ , and 150  $\mu\text{g}/\text{mL}$ ) on mitochondrial network morphology. (A) Representative images of control (unexposed) cells and cells treated with DMSO, 7.5  $\mu\text{g}/\text{mL}$  3R4F reference cigarette smoke, and 7.5  $\mu\text{g}/\text{mL}$ , 37.5  $\mu\text{g}/\text{mL}$ , 150  $\mu\text{g}/\text{mL}$  THS 2.2 aerosol TPM. Asterisks indicate for disrupted mitochondrial network (more separated from network and round mitochondria). Red, mitochondria; blue, nuclei. Scale bar represents 5  $\mu\text{m}$ . (B) The graph shows quantitative changes in the morphology of the mitochondrial network.



network fragmentation only in 10% of cells. Higher concentrations (37.5 and 150  $\mu\text{g}/\text{mL}$ ) of TPM from THS 2.2 aerosol evoked gradual increase in the content of cells with fragmented mitochondria (32 and 50%, respectively).

To examine the plasticity of mitochondrial dynamics, we assessed mitochondrial morphology under conditions of nutrient deprivation – cells starvation (incubation in PBS). Minor stress, such as starvation, induced mitochondrial hyperfusion in control cells and in cells treated with DMSO or 7.5  $\mu\text{g}/\text{mL}$  and 37.5  $\mu\text{g}/\text{mL}$  THS 2.2 TPM, but only to a slight degree in cells treated with 7.5  $\mu\text{g}/\text{mL}$  3R4F TPM or 150  $\mu\text{g}/\text{mL}$  THS 2.2 TPM (marked by white arrows in Fig. 5). Fig. 5 (A and B) shows the changes in the mitochondrial network expressed as an increased proportion of tubular-shaped organelles. The graph in Fig. 5 (C and D) shows quantitative changes in the structure of the mitochondrial network both before and after starvation, respectively. Chronic exposure (12 weeks) of BEAS-2B cells to TPM from 3R4F (7.5  $\mu\text{g}/\text{mL}$ ) cigarette smoke led to fragmentation of the mitochondrial network in almost entire population of cells (85%), whereas such exposure of cells to TPM from THS 2.2 aerosol had only minimal impact on mitochondrial network morphology. Under the nutrient deprivation conditions, incubation of BEAS-2B cells with 7.5  $\mu\text{g}/\text{mL}$  of TPM from 3R4F cigarette smoke and highest concentration (150  $\mu\text{g}/\text{mL}$ ) of TPM from THS 2.2 aerosol for 12 weeks, resulted in fragmentation of mitochondrial network in 52 and 67% of cell population, respectively. The rest of the cell population had partially fragmented mitochondria.

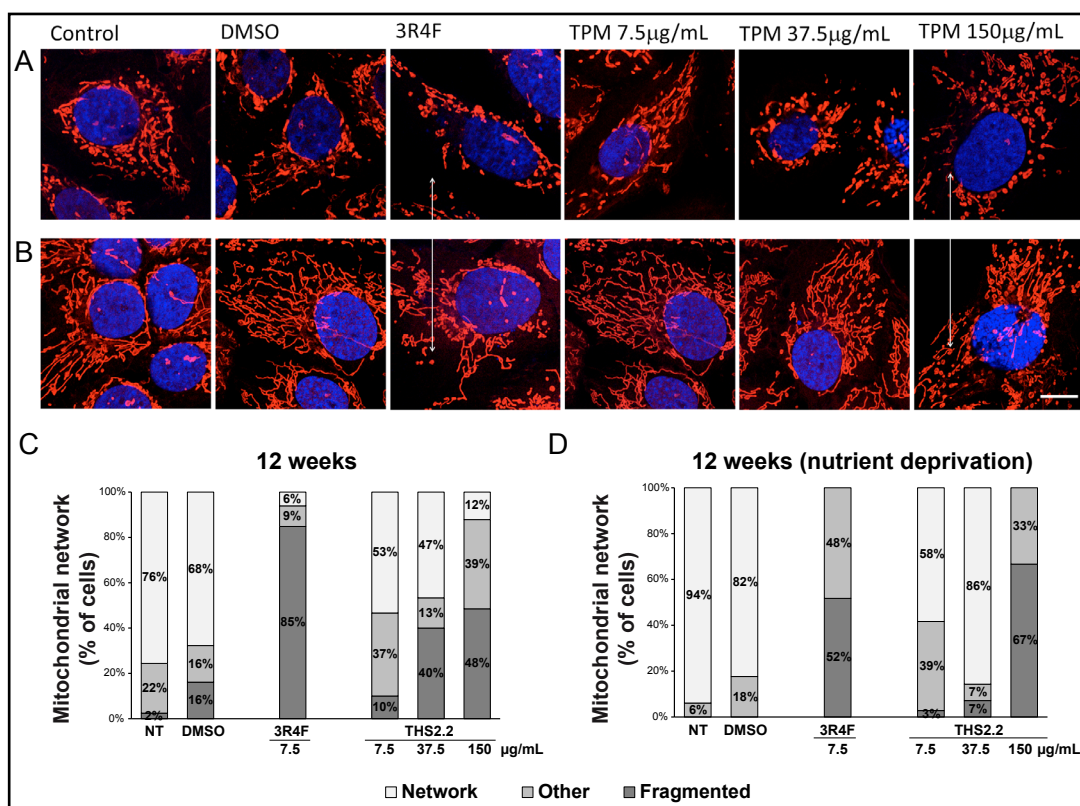


**Fig. 5.** Effects of a 12-week exposure of BEAS-2B cells to TPM from 3R4F reference cigarette smoke (7.5  $\mu\text{g}/\text{mL}$ ) and THS 2.2 aerosol (7.5  $\mu\text{g}/\text{mL}$ , 37.5  $\mu\text{g}/\text{mL}$ , and 150  $\mu\text{g}/\text{mL}$ ) on mitochondrial network morphology (A) and after 24h of starvation (B). Representative images of control (unexposed) cells and cells treated with DMSO, 7.5  $\mu\text{g}/\text{mL}$  3R4F reference cigarette smoke, and 7.5  $\mu\text{g}/\text{mL}$ , 37.5  $\mu\text{g}/\text{mL}$ , 150  $\mu\text{g}/\text{mL}$  THS 2.2 aerosol TPM. Arrows indicate those cells in which the mitochondrial network is not completely connected. Red, mitochondria; blue, nuclei. Scale bar represents 10  $\mu\text{m}$ . (C, D) The graphs show quantitative changes in the morphology of the mitochondrial network.

*Effects of short- and chronic exposure to TPM from 3R4F cigarette smoke and from THS 2.2 aerosol on levels of mitochondrial fusion and fission proteins.* Confocal microscopy revealed changes in the mitochondrial morphology of cells exposed to TPM from 3R4F cigarette smoke and THS 2.2 aerosol (Fig. 4 and 5). Because mitochondrial network morphology and dynamics strongly depend on fusion and fission proteins, we examined the changes in the levels of these proteins following exposure. The levels of proteins responsible for the fusion of the outer mitochondrial membrane (Mfn1 and Mfn2) remained unchanged after a one-week treatment with TPM from 3R4F cigarette smoke or THS 2.2 aerosol compared with levels in DMSO-exposed cells (Fig. 6A and B). A 12-week exposure to 7.5 µg/mL 3R4F TPM decreased the levels of Mfn1 and Mfn2 by  $22 \pm 3\%$  (n=4; Fig. 6A) and  $30 \pm 9\%$  (n=4; Fig. 6B), respectively.

OPA1 is another protein that mediates the fusion of the inner mitochondrial membrane, and its activity is regulated by protease-driven proteolysis. This proteolytic processing leads to the formation of long (L-OPA1) and short (S-OPA1) isoforms of the protein. Accumulation of short isoforms has been correlated with mitochondrial fragmentation, while the long isoforms promote fusion [29]. Changes in mitochondrial functionality, such as a decrease in membrane potential, can cause extensive proteolytic cleavage of L-OPA1, which then shifts the L-OPA1/S-OPA1 ratio toward the short isoforms, correlating with strong fragmentation of the mitochondrial network [30]. Although overall levels of OPA1 did not change following a one-week exposure (Fig. 6C), the L-OPA1/S-OPA1 ratio increased by  $45 \pm 10\%$  in cells exposed to 3R4F (7.5 µg/mL) TPM (n=3; Fig. 6D). Similarly, the highest concentration of TPM from THS 2.2 (150 µg/mL) aerosol also caused an increase in the L-OPA1/S-OPA1 ratio but without reaching statistical significance. Following a 12-week exposure to 37.5 µg/mL THS 2.2 TPM, the L-OPA1/S-OPA1 ratio decreased by  $11 \pm 3\%$  in comparison with the ratio in DMSO-exposed cells (n=3), while exposure to the highest concentration of THS 2.2 (150 µg/mL) increased OPA1 levels by  $17 \pm 8\%$  (n=3; Fig. 6D).

One of the main proteins responsible for mitochondrial fission is Drp1; its activity is regulated by a series of post-translational modifications, such as phosphorylation of Ser616 in the variable domain [31]. Levels of Drp1 phosphorylated at serine 616 (pDrp1-S616) increased by  $90 \pm 11\%$  in cells exposed for one week to 7.5 µg/mL 3R4F TPM (n=3) and by  $40 \pm 22\%$  in cells treated with 150 µg/mL THS 2.2 TPM (n=3; Fig. 7B). A similar effect was observed for the ratio of pDrp1-S616 to total Drp1, which was higher in cells exposed to 7.5 µg/mL 3R4F TPM and 150 µg/mL THS 2.2 TPM than in DMSO-exposed cells ( $52 \pm 2\%$ ; n=3 and  $55 \pm 17\%$ ; n=3, respectively; Fig. 7C). Total Drp1 levels increased by  $24 \pm 6\%$  in cells exposed for one week to 7.5 µg/mL 3R4F TPM (n=3; Fig. 7A). Interestingly, a 12-week exposure resulted in an opposite effect, inducing a slight decrease in the pDrp1-S616/Drp1 ratio of  $11 \pm 3\%$  (n=3) and  $20 \pm 5\%$  (n=3) in cells exposed to 7.5 µg/mL 3R4F TPM and 150 µg/mL THS 2.2 TPM, respectively, in comparison with the ratio in DMSO-treated cells (Fig. 7B).

The process of fission also depends on small proteins localized on the outer mitochondrial membrane, Fis1 and Mff, which promote mitochondrial fission by recruiting Drp1 [16]. In BEAS-2B cells exposed to TPM for one-week, Fis1 levels appeared higher than in DMSO-treated cells. A 12-week exposure to 7.5 µg/mL 3R4F TPM and 150 µg/mL THS 2.2 TPM caused a slight decrease (by 10%) of Fis1 levels in DMSO-exposed cells, but the effect was not statistically significant (Fig. 7D). A one-week exposure to TPM from 150 µg/mL THS 2.2 TPM decreased Mff levels by  $34 \pm 17\%$  (n=4). A similar tendency was observed in cells exposed to 7.5 µg/mL 3R4F TPM, with borderline significance (Fig. 7E). The 12-week exposure increased Mff levels by  $23 \pm 11\%$  in cells exposed to 3R4F TPM (n=4) and by  $18 \pm 13\%$  in cells exposed to the lowest concentration of THS 2.2 TPM (7.5 µg/mL; n=4), in comparison with Mff levels in DMSO-treated cells (Fig. 7E).

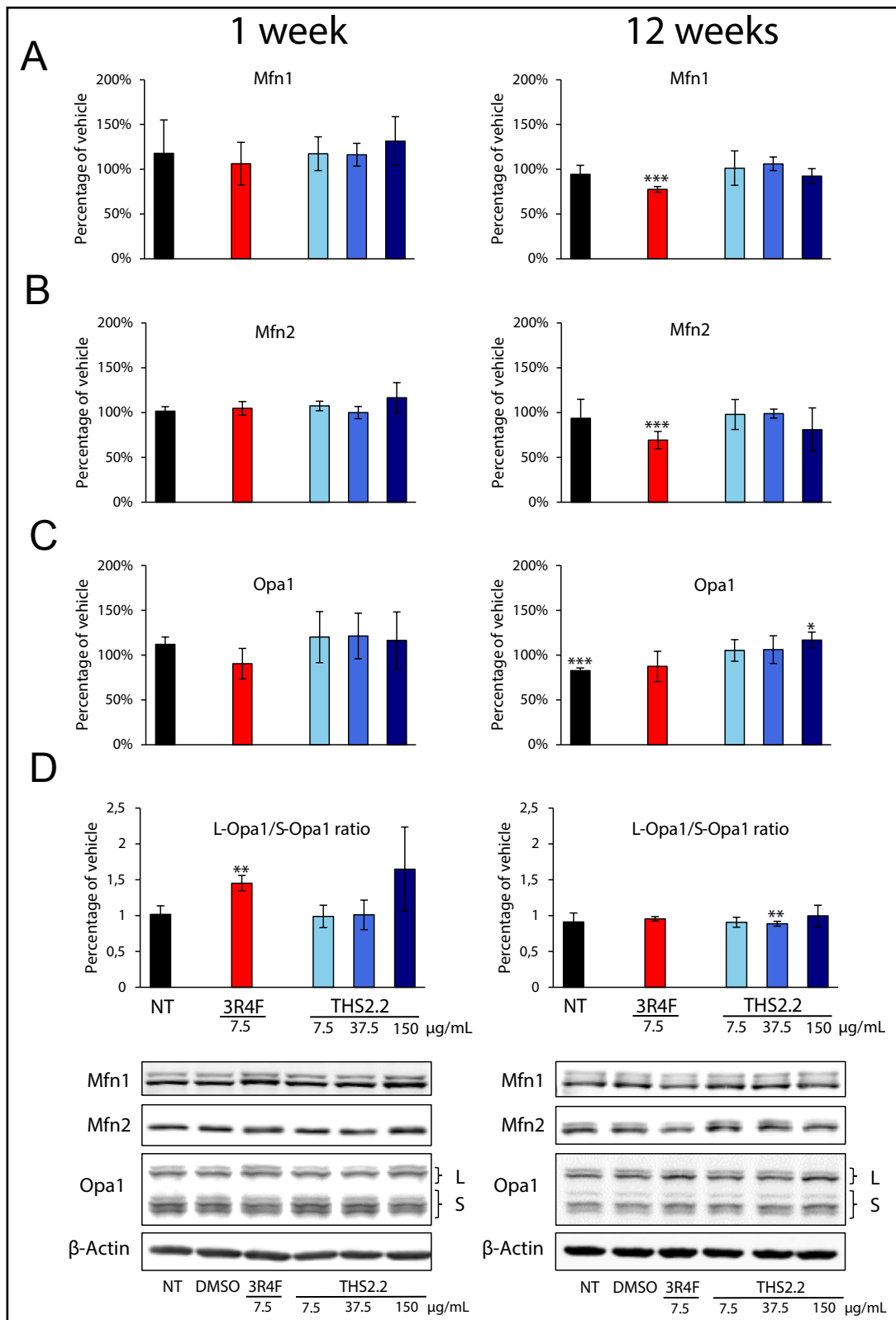


**Fig. 6.** Effects of one- and 12-week exposures of BEAS-2B cells to TPM from 3R4F reference cigarette smoke (7.5  $\mu\text{g}/\text{mL}$ ) and THS 2.2 aerosol (7.5  $\mu\text{g}/\text{mL}$ , 37.5  $\mu\text{g}/\text{mL}$ , and 150  $\mu\text{g}/\text{mL}$ ) on levels of key fusion proteins. (A) Mfn1, (B) Mfn2, (C) OPA1, (D) ratio of L-OPA1 to S-OPA1 isoforms. Values represent the means  $\pm$  SD from at least three independent experiments, with representative images of the corresponding Western blots;  $\beta$ -actin was used as the loading control. \* $p < 0.05$ , \*\* $p < 0.01$ , \*\*\* $p < 0.001$  compared with vehicle (DMSO)-treated cells. NT, non-treated (control) cells. L - long isoforms of Opa1, S - short isoforms of Opa1.

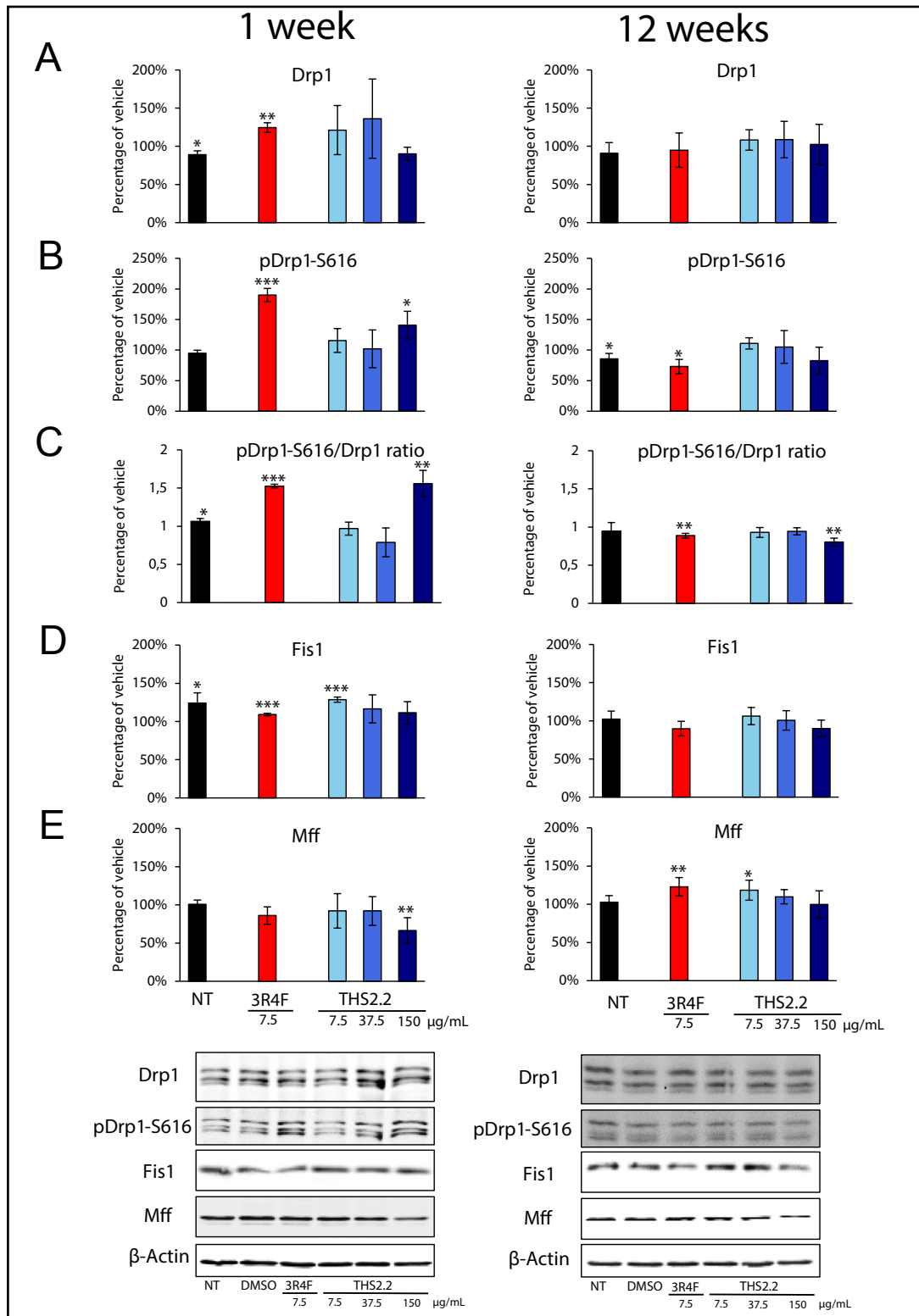


**Fig. 7.** Effects of one- and 12-week exposures of BEAS-2B cells to TPM from 3R4F reference cigarette smoke (7.5  $\mu\text{g/mL}$ ) and THS 2.2 aerosol (7.5  $\mu\text{g/mL}$ , 37.5  $\mu\text{g/mL}$ , and 150  $\mu\text{g/mL}$ ) on levels of mitochondrial fission proteins. (A) Drp1, (B) Drp1 protein phosphorylated at Ser 616 (pDrp1-S616), (C) ratio of pDrp1-S616 to total Drp1, (D) Fis1, and (E) Mff. Values represent the means  $\pm$  SD from at least three independent experiments, with representative images of the corresponding Western blots;  $\beta$ -actin was used as the loading control. \* $p < 0.05$ , \*\* $p < 0.01$ , \*\*\* $p < 0.001$  compared with vehicle (DMSO)-treated cells. NT, non-treated (control) cells.

### *Mitochondrial mass and biogenesis*

In addition to shaping the mitochondrial network, fusion and fission processes are responsible for mitochondrial turnover [32], which affects mitochondrial mass. Changes in mitochondrial mass are an early indicator of activation or inhibition of mitochondrial biogenesis.

Mitochondrial mass, measured using the MitoTracker™ Green fluorescent probe, increased in BEAS-2B cells exposed for one week to 7.5 µg/mL 3R4F TPM and to 150 µg/mL THS 2.2 TPM by  $9 \pm 6\%$  (n=4) and  $20 \pm 10\%$  (n=3), respectively. In contrast, the 12-week exposure decreased mitochondrial mass by  $13 \pm 9\%$  (n=5) and by  $18 \pm 7\%$  (n=5), respectively (Fig. 8A).

Mitochondrial biogenesis depends on signaling cascades that activate transcription factors and lead to the expression of genes encoding proteins involved in mitochondrial formation and functionality. NRF1 and NRF2 are regulators of gene expression that modulate the transcription of key mitochondrial enzymes. Levels of NRF1 in cells exposed to the highest concentration of TPM from THS 2.2 aerosol for one week were lower by  $44 \pm 12\%$  than those in DMSO-treated cells (n=3). A similar tendency was observed for cells treated with TPM from 3R4F cigarette smoke, but this result did not reach statistical significance. In contrast, a 12-week exposure to 3R4F TPM increased NRF1 levels by  $63 \pm 38\%$  (n=3), while NRF1 levels in cells exposed to TPM from THS 2.2 aerosol remained unchanged (Fig. 8B).

Levels of NRF2 decreased after a one-week exposure to TPM from 3R4F cigarette smoke and the highest concentration of TPM from THS 2.2 aerosol by  $67 \pm 7\%$  (n=4) and  $67 \pm 16\%$  (n=4), respectively. The 12-week exposure resulted in the opposite effect: NRF2 levels increased in comparison with levels in DMSO-treated cells. Exposure to 7.5 µg/mL and 37.5 µg/mL THS 2.2 TPM increased NRF2 levels by  $120 \pm 26\%$  (n=4) and  $158 \pm 26\%$  (n=4), respectively. The strongest effect was observed for cells exposed to TPM from 3R4F cigarette smoke and 150 µg/mL TPM from THS 2.2 aerosol, where NRF2 levels increased by  $866 \pm 392\%$  (n=4) and  $1,037 \pm 205\%$  (n=4), respectively (Fig. 8C).

NRF1 and NRF2 have also been shown to control the expression of mitochondrial transcription factor A (TFAM), a major regulator of mitochondrial DNA transcription and replication [33]. TFAM levels decreased following a one-week exposure to TPM from 3R4F cigarette smoke and TPM from THS 2.2 aerosol (150 µg/mL) by  $32 \pm 14\%$  (n=3) and  $31 \pm 19\%$  (n=3), respectively. After 12 weeks of exposure, TFAM levels were only altered in cells exposed to 7.5 µg/mL THS 2.2 TPM; levels increased by  $32 \pm 3\%$  (n=3) in comparison with levels in DMSO-treated cells (Fig. 8D).

A summary of all investigated parameters can be found in Table 1.

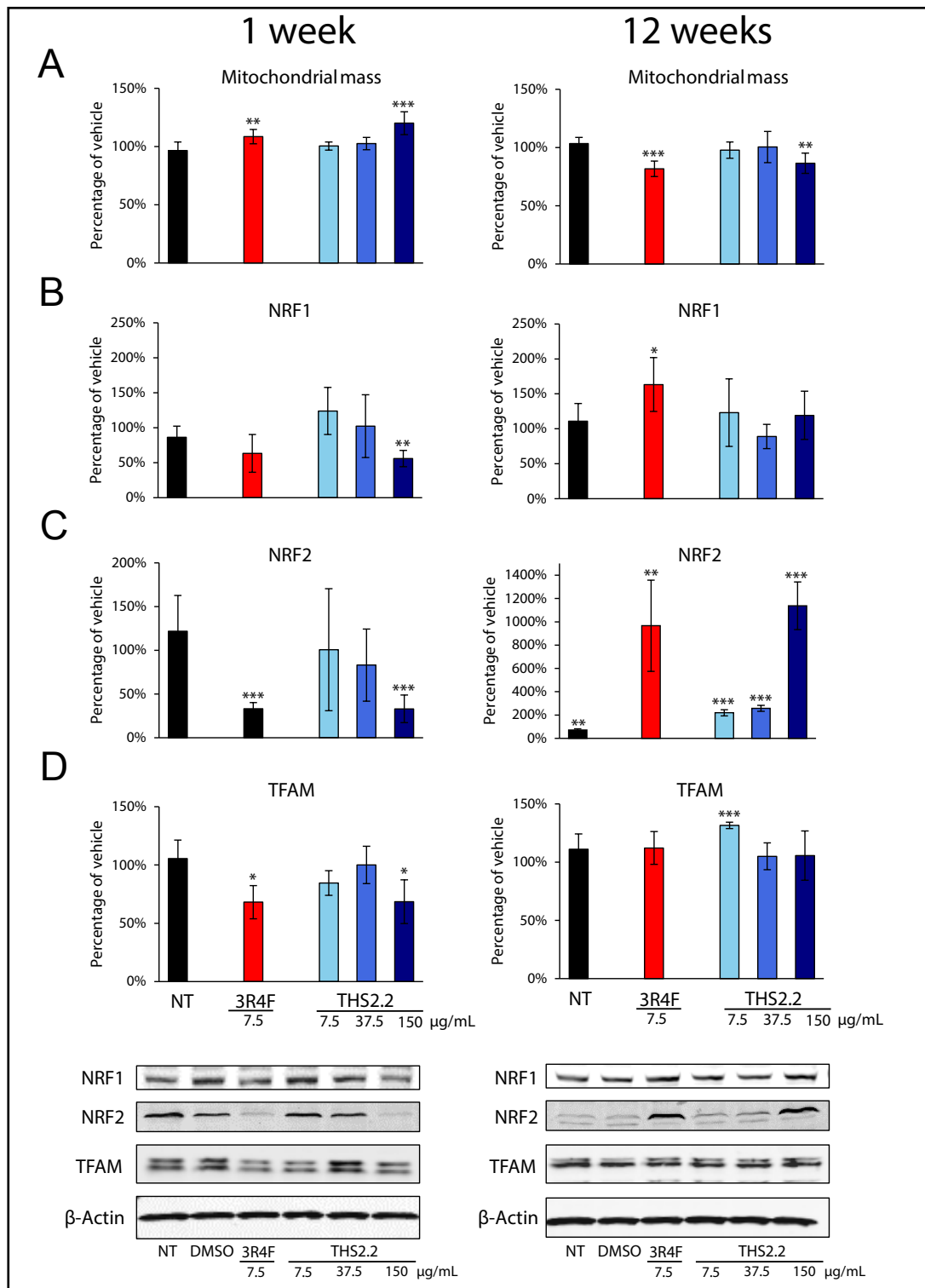


**Fig. 8.** Effects of one- and 12-week exposures of BEAS-2B cells to TPM from 3R4F reference cigarette smoke (7.5 µg/mL) and THS 2.2 aerosol (7.5 µg/mL, 37.5 µg/mL, and 150 µg/mL) on mitochondrial mass and levels of key biogenesis-regulating proteins. (A) Mitochondrial mass measured using a MitoTracker™ Green fluorescent probe, (B) NRF1, (C) NRF2, and (D) TFAM. Values represent the means ± SD from at least three independent experiments, with representative images of the corresponding Western blots; β-actin was used as the loading control. \* $p < 0.05$ , \*\* $p < 0.01$ , \*\*\* $p < 0.001$  compared with vehicle (DMSO)-treated cells. NT, non-treated (control) cells.

**Table 1.** Summary of biological outcome of one- and 12-week exposures of BEAS-2B cells to TPM from 3R4F reference cigarette smoke (7.5 µg/mL) and THS 2.2 aerosol (7.5 µg/mL, 37.5 µg/mL, and 150 µg/mL) in comparison to vehicle (DMSO)-exposed cells

Exposure	1 week				12 weeks			
	3R4F TPM 7.5 µg/ml	7.5 µg/ml	THS 2.2 TPM 37.5 µg/ml	150 µg/ml	3R4F TPM 7.5 µg/ml	7.5 µg/ml	THS 2.2 TPM 37.5 µg/ml	150 µg/ml
Parameter								
Cell morphology	slight changes	no	no	slight changes	different	no	no	different
Mitochondrial network	more fragmented	no	more fragmented	more fragmented	fragmented	no	fragmented	fragmented
Mitochondrial network after starvation	fragmented	fused	fused	fragmented	fragmented	fused	fused	fragmented
ΔΨ	-	-	-	-	-	-	-	-
Ca <sup>2+</sup>	↑	-	-	↑	↓	-	-	↓
	Mitochondrial fusion proteins							
MFN1	-	-	-	-	↓	-	-	-
MFN2	-	-	-	-	↓	-	-	-
L-OPA1/S-OPA1 ratio	↑	-	-	-	-	-	↓	-
	Mitochondrial fission proteins							
DRP1	↑	-	-	-	-	-	-	-
pDRP1/DRP1 ratio	↑	-	-	↑	↓	-	-	↓
FIS1	↑	↑	-	-	-	-	-	-
MFF	-	-	-	↓	↑	↑	-	-
	Mitochondrial biogenesis							
Mitochondrial mass	↑	-	-	↑	↓	-	-	↓
NRF1	↓	-	-	↓	↑	-	-	-
NRF2	↓↓↓	-	-	↓↓↓	↑↑↑	↑	↑	↑↑↑
TFAM	↓	-	-	↓	-	↑	-	-

## Discussion

The aim of this work was to compare the functioning of mitochondria and repercussion of mitochondrial stress signaling in response to short-term (1 week) and chronic (12 weeks) stress induced by TPM from 3R4F reference cigarette smoke or 3 different concentrations of TPM generated from THS 2.2 aerosol in BEAS-2B cells. In our previous study where we evaluated main mitochondrial parameters (i.a. ATP production, oxygen consumption rate, ROS generation), we demonstrated that exposure to 3R4F or a 20-fold higher concentration of THS 2.2 TPM leads to alterations in mitochondrial respiratory chain function and oxidative stress in BEAS-2B cells [34]. Continuing this research, we focus here on the influence of TPM from 3R4F cigarette smoke and THS 2.2 aerosol on mitochondrial morphology and dynamics in the same *in vitro* model. Disturbances of mitochondrial dynamics, especially during stress conditions, evoke changes in the morphology of the mitochondrial network, oxidative stress, and calcium homeostasis, affecting many cellular functions. As the balance of mitochondrial fusion and fission processes is highly sensitive to environmental changes, disturbances of mitochondrial morphology could have an impact on mitochondrial function and mitochondria-dependent cellular events [35].

The influence of short-term exposure to TPM from 3R4F cigarette smoke and THS 2.2 aerosol was noticeable during proliferation. Results show that TPM from 3R4F cigarette smoke and a 20-fold higher concentration of TPM from THS 2.2 aerosol impacted the cellular growth rate in the first week of exposure. The observed changes in proliferation rate have a profound impact on the morphology of BEAS-2B cells. 3R4F TPM-exposed cells as well as cells

exposed to a 20-fold higher concentration of THS 2.2 TPM had irregular, elongated shapes with visual clusters of thick filaments. Changes of cell morphology and arrest of cell cycle are early indicators of profound metabolic changes that are often correlated with disturbed mitochondrial function. The impact of TPM from both 3R4F cigarette smoke and THS 2.2 aerosol on mitochondrial physiology in BEAS-2B cells has already been described in our previous work [34]. Here we extended our research to measure mitochondrial membrane potential and cytosolic calcium levels. We did not observe statistically significant changes in mitochondrial membrane potential during the short-term and chronic TPM exposure, although a lower mitochondrial membrane potential in cells exposed to cigarette smoke extract was previously reported [36–38]. In most cases, these observations were made after much shorter exposure duration in comparison to the conditions implemented in our study. It is possible that during chronic exposure, the mitochondrial membrane potential in BEAS-2B cells is already rebuilt.

Despite the fact that mitochondrial membrane potential remained unchanged after one-week exposure to TPM, the level of cytosolic calcium was elevated in cells exposed to TPM from 3R4F cigarette smoke and a 20-fold higher concentration of THS 2.2 TPM. Interestingly, chronic TPM exposure decreased intracellular calcium levels below the level seen in the control BEAS-2B cells. Increased intracellular calcium levels may be a consequence of impaired buffering of calcium ions by mitochondria. This function of mitochondria is strongly dependent on its proper positioning in proximity to other cellular structures, especially the endoplasmic reticulum and cell membrane [39]. The proper positioning of mitochondria strongly depends on processes regulating their morphology (fission and fusion) as well as the coordinated transport of these organelles within the cell.

The typical mitochondrial network in BEAS-2B cells is mostly composed of elongated, tubular mitochondria distributed evenly within the cell. Short exposure to TPM from 3R4F cigarette smoke and a 20-fold higher concentration of THS 2.2 TPM caused visible changes in the morphology of the mitochondrial network, which became more fragmented. This fragmentation was especially visible when cells were deprived of energy supply during starvation. Fragmentation of mitochondrial network under stress conditions is a well-documented phenomenon that has been observed in human airway smooth muscle cells, primary human bronchial epithelial cells and retinal pigment epithelial cells exposed to cigarette smoke extract [36, 40–42]. Generally, stress-induced mitochondrial fragmentation is related to disturbances in mitochondrial functioning, such as decreased mitochondrial membrane potential, ATP production and oxidative stress [15, 43–45]. According to our previous study, no changes were observed in cytosolic reactive oxygen species (ROS) levels in TPM-exposed BEAS-2B cells, but mitochondrial superoxide levels were found to be increased, particularly in cells exposed to TPM from 3R4F cigarette smoke and a 20-fold higher concentration of THS 2.2. Moreover, the observed increase in mitochondrial superoxide level arose mainly due to electron leaks during mitochondrial electron transport chain activity [34]. It is possible that the observed oxidative stress in TPM-exposed BEAS-2B cells is also responsible for the increased fragmentation of mitochondria. A study performed in cigarette smoke extract-exposed human bronchial epithelial cells showed that ROS derived from mitochondria contribute, at least in part, to mitochondrial fragmentation [36]. Moreover, ROS-related disturbances of mitochondrial dynamics and an increased fission process might also lead to impaired calcium buffering in BEAS-2B cells.

Mitochondrial fragmentation is not a random process; it is tightly regulated by proteins responsible for mitochondrial dynamics. Short-term exposure of BEAS-2B cells to TPM from 3R4F cigarette smoke and a 20-fold higher concentration of THS 2.2 TPM strongly elevated the levels of pDrp1-S616 compared with the vehicle-treated cells. Increased levels of pDrp1-S616 protein results in its translocation from the cytoplasm to the mitochondria and leads to fragmentation processes [31]. Son et al. demonstrated a strong increase in pDrp1-S616 levels in BEAS-2B cells as early as 16 hours after exposure to cigarette smoke. This was correlated with impaired mitochondrial membrane potential and increased mitochondrial ROS (mtROS) production [37]. Similar results were obtained for pulmonary

epithelial cells, where cigarette smoke extract promoted mtROS production and increased pDrp1-S616 protein levels [42]. The fragmentation of the mitochondrial network is regulated by the opposite process: mitochondrial fusion. For example, during starvation, mitochondria are protected from excessive degradation by mitochondrial elongation in fusion processes, which are regulated by mitofusins and OPA1 proteins [46]. Fragmentation of long isoforms of OPA1 by specific mitochondrial proteases is activated by decreased mitochondrial membrane potential and shifts the fusion/fission balance toward the fission process [29]. We observed changes in the ratio of long to short isoforms towards the long isoform of the inner mitochondrial membrane fusion protein OPA1. This suggests the activation of the process opposite to the Drp1-driven fragmentation of mitochondria in order to limit excessive fragmentation and degradation of these organelles.

Chronic exposure of BEAS-2B to TPM from 3R4F cigarette smoke and a 20-fold higher concentration of THS 2.2 TPM strongly decreased the levels of pDrp1-S616 protein below the level of vehicle-exposed control. Levels of mitochondrial fusion proteins (Mfn1 and Mfn2) were exclusively lowered in these cells. Mfn2 is not only responsible for the fusion of mitochondrial membranes but also plays an important role in the regulation of cellular bioenergetic metabolism [47]. It has been shown that downregulation of Mfn2 leads to a significant extracellular acidification rate (ECAR), which is an indicator of robust glycolysis [35]. In our previous work, we showed that chronic exposure of BEAS-2B cells to TPM from 3R4F cigarette smoke elevates both ECAR and oxygen consumption rate, indicating increased glycolysis and mitochondrial function [34]. These data may indicate that there is a correlation between mitochondrial morphology regulation and changes in the energy production during the adaptation process which is regulated by mitochondrial stress signaling (retrograde signaling).

Mitochondrial dynamics are essential in the process of mitochondrial turnover, allowing for selective degradation of dysfunctional mitochondria and biogenesis of a new pool of these organelles. Biogenesis of mitochondria, particularly under stress conditions, is often reflected by an increase in their mass. We observed higher mitochondrial mass in BEAS-2B cells exposed to TPM from 3R4F cigarette smoke and a 20-fold higher concentration of THS 2.2 TPM in comparison to vehicle-exposed cells. Surprisingly, levels of proteins engaged in mitochondrial biogenesis (NRF1, NRF2, TFAM) were decreased in those cells. It has been shown that exposure of primary lung cells to cigarette smoke extract leads to impaired degradation of mitochondria and perinuclear accumulation of damaged mitochondria, oxidative stress, and induction of DNA damage [48]. A similar situation may take place during the exposure of BEAS-2B cells to TPM. van der Toorn et al. showed increased levels of gamma H2AX, a marker of DNA double-strand breaks in BEAS-2B cells exposed to TPM from 3R4F cigarette smoke and THS 2.2 aerosol [49]. Even though the mitochondrial mass was decreased in cells subjected to chronic exposure to 3R4F TPM, the level of the biogenesis-related protein NRF1 was higher in comparison to vehicle-exposed cells. Upon chronic exposure to TPM, we observed an increase in NRF2 protein level, which was extremely strong in cells exposed to 3R4F TPM and a 20-fold higher concentration of THS 2.2 TPM. One of the most important functions of the NRF2 protein is the protection against oxidative stress through activation of antioxidant defense and cytoprotective genes. Different studies show that cigarette smoke extract enhances expression of NRF2 and its target genes, and this may be one of the key cytoprotective mechanisms [41, 50]. Moreover, Lin et al. suggested that antioxidant NRF2 is up-regulated by the ROS/p38 signaling pathway in cigarette smoke extract-exposed BEAS-2B cells [51].

## Conclusion

Our study revealed, that short term (1 week) exposure to components of cigarette smoke evoke mitochondrial stress in bronchial epithelial cells, which manifests in mitochondrial network fragmentation, altered levels of proteins involved in mitochondrial dynamics and biogenesis as well as in general cellular stress symptoms such as slower proliferation, cell morphology changes or cytosolic  $Ca^{2+}$  elevation.

In turn, upon long-term (12 weeks) exposure to the analyzed TPMs we have observed signs of cellular adaptation: mitochondrial network fragmentation was less pronounced and many parameters (such as DRP1 phosphorylation, levels of NRF1 and NRF2 transcription factors, mitochondrial mass or cytosolic  $Ca^{2+}$ ) were affected in opposite way than observed after 1 week exposure.

Mitochondrial stress usually leads to changes in mitochondrial dynamics and finally can lead to cell adaptation or cell senescence [14, 48]. Chronic exposure of cells to TPM leads to cellular crisis, which probably eliminates part of the cells from the population due to irreparable damage. Mitochondria in cells which survived this crisis undergo functional and phenotypic changes allowing them to adapt to the chronic stress caused by toxicants contained in the TPM [49].

Comparison of the effects of TPM from 3R4F reference cigarette and from THS 2.2 aerosol, a candidate modified risk tobacco product, revealed that to get similar extent of changes in mitochondrial dynamics and biogenesis, TPM from THS 2.2 had to be applied in 20-times higher concentration than TPM from 3R4F. Reducing the formation of constituents identified as toxicants in THS 2.2 aerosol may explain why mitochondrial dynamics, architecture and biogenesis were not impacted at comparable doses of cigarette smoke.

## Acknowledgements

The authors are grateful to V. Biernat for specialist technical assistance.

### *Funding Sources*

This research was funded by Philip Morris International.

### *Author Contributions*

Conceptualization, J.S., J.H., M.R.W. and M.T.; methodology, J.W., D.M. and J.S.; investigation, J.W., D.M., K.D., B.M., M.P., J.Sz and S.J.; writing—original draft preparation, J.W., J.S., D.M.; writing—review and editing, J.W., J.S., D.M., M.C.P., S.J., K.L., J.H. and M.T.; supervision, J.S., M.T., M.C.P., M.R.W., J.D. and J.H.; funding acquisition, J.S. and J.D.

## Disclosure Statement

Philip Morris International is the sole source of funding and sponsor of this research.

Stephanie Johnne, Karsta Luettich, Manuel C Peitsch, Julia Hoeng, and Marco van der Toorn are employees of Philip Morris International.

## References

- 1 Dela Cruz CS, Tanoue LT, Matthay RA: Lung Cancer: Epidemiology, Etiology, and Prevention. *Clin Chest Med* 2011;3:605–644.
- 2 Vestbo J, Hurd SS, Agustí AG, Jones PW, Vogelmeier C, Anzueto A, Barnes PJ, Fabbri LM, Martinez FJ, Nishimura M, Stockley RA, Sin DD, Rodriguez-Roisin R: Global strategy for the diagnosis, management, and prevention of chronic obstructive pulmonary disease: GOLD executive summary. *Am J Respir Crit Care Med* 2013;187:347–365.
- 3 Talhout R, Schulz T, Florek E, van Benthem J, Wester P, Opperhuizen A: Hazardous compounds in tobacco smoke. *Int J Environ Res Public Health* 2011;8:613–628.
- 4 Zhao J, Zhang J, Yu M, Xie Y, Huang Y, Wolff DW, Abel PW, Tu Y: Mitochondrial dynamics regulates migration and invasion of breast cancer cells. *Oncogene* 2013;32:4814–4824.
- 5 Galluzzi L, Kepp O, Trojel-Hansen C, Kroeme G: Mitochondrial control of cellular life, stress, and death. *Circ Res* 2012;111:1198–1207.
- 6 Scheffler IE: *Mitochondria*, ed 2. WILEY-LISS, Hoboken, NJ, 2008.
- 7 Kotiadis VN, Duchen MR, Osellame LD: Mitochondrial quality control and communications with the nucleus are important in maintaining mitochondrial function and cell health. *Biochim Biophys Acta* 2014;1840:1254–1265.
- 8 Suomalainen A, Battersby BJ: Mitochondrial diseases: the contribution of organelle stress responses to pathology. *Nat Rev Mol Cell Biol* 2018;19:77–92.
- 9 Lagouge M, Larsson NG: The role of mitochondrial DNA mutations and free radicals in disease and ageing. *J Intern Med* 2013;273:529–543.
- 10 Lund M, Melbye M, Diaz LJ, Duno M, Wohlfahrt J, Vissing J: Mitochondrial dysfunction and risk of cancer. *Br J Cancer* 2015;112:1134–1140.
- 11 Zsurka G, Kunz WS: Mitochondrial involvement in neurodegenerative diseases. *IUBMB Life* 2013;65:263–272.
- 12 Ugarte-Urbe B, García-Sáez AJ: Membranes in motion: mitochondrial dynamics and their role in apoptosis. *Biol Chem* 2014;395:297–311.
- 13 Wai T, Langer T: Mitochondrial Dynamics and Metabolic Regulation. *Trends Endocrinol Metab* 2016;27:105–117.
- 14 Yoo SM, Jung YK: A Molecular Approach to Mitophagy and Mitochondrial Dynamics. *Mol Cells* 2018;41:18–26.
- 15 Wu S, Zhou F, Zhang Z, Xing D: Mitochondrial oxidative stress causes mitochondrial fragmentation via differential modulation of mitochondrial fission-fusion proteins. *FEBS J* 2011;278:941–954.
- 16 Losón OC, Song Z, Chen H, Chan DC: Fis1, Mff, MiD49, and MiD51 mediate Drp1 recruitment in mitochondrial fission. *Mol Biol Cell* 2013;24:659–667.
- 17 Otera H, Mihara K: Molecular mechanisms and physiologic functions of mitochondrial dynamics. *J Biochem* 2011;149:241–251.
- 18 Hoppins S, Nunnari J: The molecular mechanism of mitochondrial fusion. *Biochim Biophys Acta* 2009;1793:20–26.
- 19 Song Z, Chen H, Fiket M, Alexander C, Chan DC: OPA1 processing controls mitochondrial fusion and is regulated by mRNA splicing, membrane potential, and Yme1L. *J Cell Biol* 2007;178:749–755.
- 20 Zhang K, Li H, Song Z: Membrane depolarization activates the mitochondrial protease OMA1 by stimulating self-cleavage. *EMBO Rep* 2014;15:576–585.
- 21 Szczepanowska J, Malinska D, Wieckowski MR, Duszyński J: Effect of mtDNA point mutations on cellular bioenergetics. *Biochim Biophys Acta* 2012;1817:1740–1746.
- 22 Pratte P, Cosandey S, Goujon Ginglinger C: Investigation of solid particles in the mainstream aerosol of the Tobacco Heating System THS2.2 and mainstream smoke of a 3R4F reference cigarette. *Hum Exp Toxicol* 2017;36:1115–1120.
- 23 Schaller JP, Keller D, Poget L, Pratte P, Kaelin E, McHugh D, Cudazzo G, Smart D, Tricker AR, Gautier L, Yerly M, Reis Pires R, Le Bouhellec S, Ghosh D, Hofer I, Garcia E, Vanscheeuwijck P, Maeder S: Evaluation of the Tobacco Heating System 2.2. Part 2: Chemical composition, genotoxicity, cytotoxicity, and physical properties of the aerosol. *Regul Toxicol Pharmacol* 2016;81:S27–S47.

- 24 Rodgman A, Perfetti TA: The chemical components of tobacco and tobacco smoke, ed 2. CRC Press: Boca Raton, FL, 2013.
- 25 Thastrup O, Cullen PJ, Drøbak BK, Hanley MR, Dawson AP: Thapsigargin, a tumor promoter, discharges intracellular Ca<sup>2+</sup> stores by specific inhibition of the endoplasmic reticulum Ca<sup>2+</sup>(+)-ATPase. *Proc Natl Acad Sci U S A* 1990;87:2466–2470.
- 26 Yoshida S, Plant S: Mechanism of release of Ca<sup>2+</sup> from intracellular stores in response to ionomycin in oocytes of the frog *Xenopus laevis*. *J Physiol* 1992;458:307–318.
- 27 Szczepanowska J, Zabłocki K, Duszyński J: Influence of a mitochondrial genetic defect on capacitative calcium entry and mitochondrial organization in the osteosarcoma cells. *FEBS Lett* 2004;578:316–322.
- 28 Cribbs JT, Strack S: Reversible phosphorylation of Drp1 by cyclic AMP-dependent protein kinase and calcineurin regulates mitochondrial fission and cell death. *EMBO Rep* 2007;8:939–944.
- 29 Griparic L, Kanazawa T, van der Bliek AM: Regulation of the mitochondrial dynamin-like protein Opa1 by proteolytic cleavage. *J Cell Biol* 2007;178:757–764.
- 30 Anand R, Wai T, Baker MJ, Kladt N, Schauss AC, Rugarli E, Langer T: The i-AAA protease YME1L and OMA1 cleave OPA1 to balance mitochondrial fusion and fission. *J Cell Biol* 2014;204:919–929.
- 31 Chang C-R, Blackstone C: Dynamic regulation of mitochondrial fission through modification of the dynamin-related protein Drp1. *Ann NY Acad Sci* 2010;1201:34–39.
- 32 Stotland A, Gottlieb RA: Mitochondrial quality control: Easy come, easy go. *Biochim Biophys Acta* 2015;1853:2802–2811.
- 33 Piantadosi CA, Suliman HB: Redox regulation of mitochondrial biogenesis. *Free Radic Biol Med* 2012;53:2043–2053.
- 34 Malinska D, Szymański J, Patalas-Krawczyk P, Michalska B, Wojtala A, Prill M, Partyka M, Drabik K, Walczak J, Sewer A, John S, Luettich K, Peitsch MC, Hoeng J, Duszyński J, Szczepanowska J, van der Toorn M, Wieckowski MR: Assessment of mitochondrial function following short- and long-term exposure of human bronchial epithelial cells to total particulate matter from a candidate modified-risk tobacco product and reference cigarettes. *Food Chem Toxicol* 2018;115:1–12.
- 35 Aravamudan B, Thompson M, Sieck GC, Vassallo R, Pabelick CM, Prakash YS: Functional Effects of Cigarette Smoke-Induced Changes in Airway Smooth Muscle Mitochondrial Morphology. *J Cell Physiol* 2017;232:1053–1068.
- 36 Hara H, Araya J, Ito S, Kobayashi K, Takasaka N, Yoshii Y, Wakui H, Kojima J, Shimizu K, Numata T, Kawaiishi M, Kamiya N, Odaka M, Morikawa T, Kaneko Y, Nakayama K, Kuwano K: Mitochondrial fragmentation in cigarette smoke-induced bronchial epithelial cell senescence. *Am J Physiol Lung Cell Mol Physiol* 2013;305:L737-746.
- 37 Son ES, Kim SH, Ryter SW, Yeo EJ, Kyung SY, Kim YJ, Jeong SH, Lee CS, Park JW: Quercetin protects against cigarette smoke extract-induced apoptosis in epithelial cells by inhibiting mitophagy. *Toxicol In vitro* 2018;48:170–178.
- 38 van der Toorn M, Rezaayat D, Kauffman HF, Bakker SJL, Gans ROB, Koëter GH, Choi AMK, van Oosterhout AJM, Slebos DJ: Lipid-soluble components in cigarette smoke induce mitochondrial production of reactive oxygen species in lung epithelial cells. *Am J Physiol Lung Cell Mol Physiol* 2009;297:L109-114.
- 39 Rizzuto R, De Stefani D, Raffaello A, Mammucari C: Mitochondria as sensors and regulators of calcium signalling. *Nat Rev Mol Cell Biol* 2012;13:566–578.
- 40 Aravamudan B, Kiel A, Freeman M, Delmotte P, Thompson M, Vassallo R, Sieck GC, Pabelick CM, Prakash YS: Cigarette smoke-induced mitochondrial fragmentation and dysfunction in human airway smooth muscle. *Am J Physiol Lung Cell Mol Physiol* 2014;306:L840-854.
- 41 Huang C, Wang JJ, Ma JH, Jin C, Yu Q, Zhang SX: Activation of the UPR protects against cigarette smoke-induced RPE apoptosis through up-regulation of Nrf2. *J Biol Chem* 2015;290:5367–5380.
- 42 Mizumura K, Cloonan SM, Nakahira K, Bhashyam AR, Cervo M, Kitada T, Glass K, Owen CA, Mahmood A, Washko GR, Hashimoto S, Ryter SW, Choi AM: Mitophagy-dependent necroptosis contributes to the pathogenesis of COPD. *J Clin Invest* 2014;124:3987–4003.
- 43 Jendrach M, Mai S, Pohl S, Vöth M, Bereiter-Hahn J: Short- and long-term alterations of mitochondrial morphology, dynamics and mtDNA after transient oxidative stress. *Mitochondrion* 2008;8:293–304.
- 44 Walczak J, Partyka M, Duszyński J, Szczepanowska J: Implications of mitochondrial network organization in mitochondrial stress signalling in NARP cybrid and Rho0 cells. *Sci Rep* 2017;7:14864.

- 45 Westermann B: Bioenergetic role of mitochondrial fusion and fission. *Biochim Biophys Acta* 2012;1817:1833–1838.
- 46 Rambold AS, Kostecky B, Lippincott-Schwartz J: Fuse or die: Shaping mitochondrial fate during starvation. *Commun Integr Biol* 2011;4:752–754.
- 47 Schrepfer E, Scorrano L: Mitofusins, from Mitochondria to Metabolism. *Mol Cell* 2016;61:683–694.
- 48 Ahmad T, Sundar IK, Lerner CA, Gerloff J, Tormos AM, Yao H, Rahman I: Impaired mitophagy leads to cigarette smoke stress-induced cellular senescence: implications for chronic obstructive pulmonary disease. *FASEB J* 2015;29:2912–2929.
- 49 van der Toorn M, Sewer A, Marescotti D, Johne S, Baumer K, Bornand D, Dulize R, Merg C, Corciulo M, Scotti E, Pak C, Leroy P, Guedj E, Ivanov N, Martin F, Peitsch M, Hoeng J, Luettich K: The biological effects of long-term exposure of human bronchial epithelial cells to total particulate matter from a candidate modified-risk tobacco product. *Toxicol In vitro* 2018;50:95–108.
- 50 Kosmider B, Messier EM, Chu HW, Mason RJ: Human alveolar epithelial cell injury induced by cigarette smoke. *PLoS One* 2011;6:e26059.
- 51 Lin XX, Yang XF, Jiang JX, Zhang SJ, Guan Y, Liu YN, Sun YH, Xie QM: Cigarette smoke extract-induced BEAS-2B cell apoptosis and anti-oxidative Nrf-2 up-regulation are mediated by ROS-stimulated p38 activation. *Toxicol Mech Methods* 2014;24:575–583.